

Supporting Information.

Iridium-Bismuth Cluster Complexes yield Bimetallic Nano-Catalysts for the Direct Oxidation of 3-Picoline to Niacin

Richard D. Adams,^{*†} Mingwei Chen,[†] Gaya Elpitiya[†], Matthew E. Potter[§] and Robert Raja^{*§}

[†]Department of Chemistry and Biochemistry, University of South Carolina, Columbia, SC, 29208.

[§]School of Chemistry, University of Southampton, Highfield, Southampton SO17 1BJ, U.K.

Experimental Details.

General Data. Reagent grade solvents were dried by the standard procedures and were freshly distilled under nitrogen prior to use. Infrared spectra were recorded on a Thermo Nicolet Avatar 360 FT-IR spectrophotometer. Mass spectrometric (MS) measurements were performed by a direct-exposure probe using electron impact ionization (EI) by using a VG 70S instrument. BiPh₃ was obtained from STREM CHEMICALS and were used without further purification. **of** Ir₃(CO)₉(μ₃-Bi), **1** was prepared according to a published procedure.¹ Product separations were performed by TLC in air on Analtech 0.25 and 0.5 mm silica gel 60 Å *F*₂₅₄ glass plates.

Synthesis of Ir₅(CO)₁₀(μ₃-Bi)₂(μ₄-Bi), **2**.

33.0 mg (0.075 mmol) of Ph₃Bi was added to 16.0 mg (0.015 mmol) of Ir₃(CO)₉(μ₃-Bi) that was dissolved in 20 mL of hexane and was heated to reflux for ~4h or until all the Ir₃(CO)₉(μ₃-Bi) is gone. The solvent was then removed *in vacuo*, and the product was then isolated by TLC eluting using a 4:1 hexane/methylene chloride solvent mixture. This yielded 15.7 mg of dark red Ir₅(CO)₁₀(μ₃-Bi)₂(μ₄-Bi), **2** (91% yield) as the only product. Spectral data for **2**: IR ν_{CO} (cm⁻¹ in CH₂Cl₂): 2095(w), 2032(s), 2022(m), 1990(w). Mass Spec. EI/MS for **2**: *m/z* = 1868, M⁺. The

isotope distribution pattern was consistent with the presence of five iridium atoms and three bismuth atoms.

Crystallographic Analyses: Dark red single crystals of **2** suitable for x-ray diffraction analyses were obtained by slow evaporation of solvent from a hexane/methylene chloride solvent mixture at -25 °C. The data crystal was glued onto the end of a thin glass fiber. X-ray intensity data were measured by using a Bruker SMART APEX CCD-based diffractometer using Mo K α radiation ($\lambda = 0.71073 \text{ \AA}$). The raw data frames were integrated with the SAINT+ program by using a narrow-frame integration algorithm.² Correction for Lorentz and polarization effects were also applied with SAINT+. An empirical absorption correction based on the multiple measurement of equivalent reflections was applied using the program SADABS. All structures were solved by a combination of direct methods and difference Fourier syntheses, and refined by full-matrix least-squares on F^2 , using the SHELXTL software package.³ All atoms were refined with anisotropic displacement parameters. Crystal data, data collection parameters, and results of the analyses are listed in Table S1. Compound **1** crystallized in the orthorhombic crystal system. The space groups $Pnma$ and $Pna2_1$ were indicated by the systematic absences in the data. $Pnma$ was selected and confirmed by the successful solution and refinement for the structure.

Table S1. Crystallographic Data for Compound 2.

Compound	2
Empirical formula	$\text{Ir}_5\text{Bi}_3\text{C}_{10}\text{O}_{10}$
Formula weight	1868.04
Crystal system	Orthorhombic
Lattice parameters	

a (Å)	16.3842(13)
b (Å)	14.3198(11)
c (Å)	9.2009(7)
α (deg)	90.00
β (deg)	90.00
γ (deg)	90.00
V (Å ³)	2158.7(3)
Space group	<i>Pnma</i>
Z value	4
ρ_{calc} (g / cm ³)	5.748
μ (Mo K α) (mm ⁻¹)	55.096
Temperature (K)	294(2)
$2\Theta_{\text{max}}$ (°)	50.06
No. Obs. ($I > 2\sigma(I)$)	1982
No. Parameters	133
Goodness of fit (GOF) ^a	0.993
Max. shift in cycle	0.000
Residuals: * R1; wR2	0.0287; 0.0831
Absorption Correction, Max/min	Multi-scan 1.000 / 0.315
Largest peak in Final Diff. Map (e ⁻ /Å ³)	1.79

$$* R = \frac{\sum_{\text{hkl}} (|F_{\text{obs}}| - |F_{\text{calc}}|)}{\sum_{\text{hkl}} |F_{\text{obs}}|}; R_w = \left[\frac{\sum_{\text{hkl}} w (|F_{\text{obs}}| - |F_{\text{calc}}|)^2}{\sum_{\text{hkl}} w F_{\text{obs}}^2} \right]^{1/2}; w = 1/\sigma^2(F_{\text{obs}}); \text{GOF} = \left[\frac{\sum_{\text{hkl}} w (|F_{\text{obs}}| - |F_{\text{calc}}|)^2}{(n_{\text{data}} - n_{\text{vari}})} \right]^{1/2}.$$

Preparation of the catalysts:

Three supports were tested in this study; MCM-41, Davison 923 mesopore and silica gel (60, 0.06-0.2mm (70-230 mesh)).

1) 37.49 mg of $\text{Ir}_3(\text{CO})_9(\mu_3\text{-Bi})$ was dissolved in benzene. To this solution, 918 mg of MCM41 support was added and mixture was slurried under nitrogen for 24h. The solvent was then slowly removed under vacuum. The solid catalyst was then preconditioned by heating under vacuum to 200 °C for a period of 2h to remove the CO ligands to yield 0.947 g amount of supported catalyst with 3% metal loading.

2) 35.28 mg amount of **2** was dissolved in 30 mL of CH_2Cl_2 . To this solution, 970 mg of MCM-41 support was added and mixture was slurried under nitrogen for 24h. The solvent was then slowly removed under vacuum. The solid catalyst was then preconditioned by heating under vacuum to 200 °C for a period of 2h to remove the CO ligands to yield 1.00 g of catalyst with 3% metal loading.

3) A pure bismuth catalyst with 3% metal loading was prepared similarly on MCM41 by thermal treatment by using a commercially obtained sample of BiPh_3 as the precursor.

4) A pure iridium catalyst with 3% metal loading was prepared similarly by using a commercially obtained sample (STREM) of $\text{Ir}_4(\text{CO})_{12}$ as the precursor.

5) Bimetallic IrBi catalysts (physical mixes) in the Ir/Bi 3/1 and 5/3 ratios were also prepared at the 3% metal loading by coimpregnation methods by slurrying solutions containing $\text{Ir}_4(\text{CO})_{12}$ and BiPh_3 in the appropriate ratios, evaporating to dryness and preconditioning by heating to 200 °C in vacuo for 2h to remove the ligands.

High Resolution Transmission Electron Imaging of the Supported Catalysts:

Scanning high resolution transmission electron microscopy (STEM) was performed at the University of South Carolina Electron Microscopy Center by using a JEOL 2100F 200kV FEG-STEM/TEM equipped with a CEOS C_s corrector on the illumination system. The geometrical

aberrations were measured and controlled to provide less than a $\pi/4$ phase shift of the incoming electron wave over the probe-defining aperture of 17.5 mrad. High angle annular dark-field (HAADF) scanning transmission electron microscopy (STEM) images were acquired on a Fischione Model 3000 HAADF detector with a camera length such that the inner cut-off angle of the detector was 50 mrad. The scanning acquisition was synchronized to the 60 Hz AC electrical power to minimize 60 Hz noise in the images and a pixel dwell time of 15.8 μs was used.

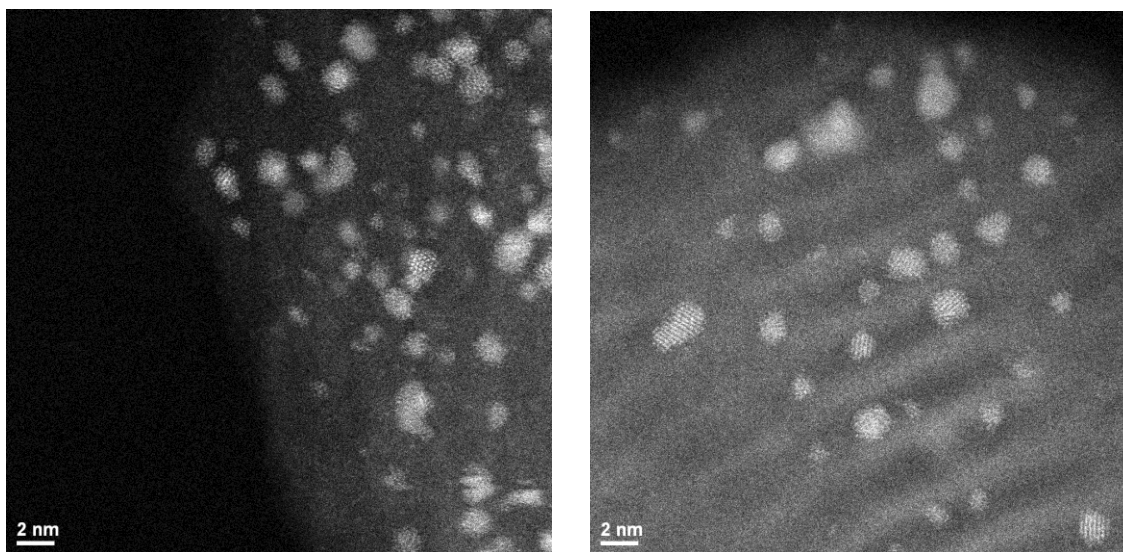


Figure S1. HAADF - HRTEM images of Ir₃Bi nanoparticles on MCM-41 before catalysis (on left, pretreated at 200 °C to remove the ligands) and after use in catalysis (on right, pretreated at 300 °C to remove the ligands).

Table S2. Seven TEM EDS Composition Analyses of Ir₃Bi catalyst on MCM-41 support: (a) before use; (b) after use.

(a) before use

Particle	Ir Atomic %	95% confidence	Bi Atomic %	95% confidence
1	78.67	±3.98	21.33	±3.66
2	80.95	±4.08	19.05	±3.76
3	75.24	±3.94	24.76	±3.62
4	75.23	±3.72	24.77	±3.44
5	75.31	±3.72	24.69	±3.42

(b) after use

Particle	Ir Atomic %	95% confidence	Bi Atomic %	95% confidence
1	74.78	±8.66	25.22	±7.96
2	91.22	±4.36	8.78	±4.00
3	80.14	±3.24	19.86	±2.98
4	80.20	±2.76	19.80	±2.54
5	78.82	±4.66	21.18	±4.30
6	82.23	±5.80	17.77	±5.34
7	86.35	±4.58	13.65	±4.20

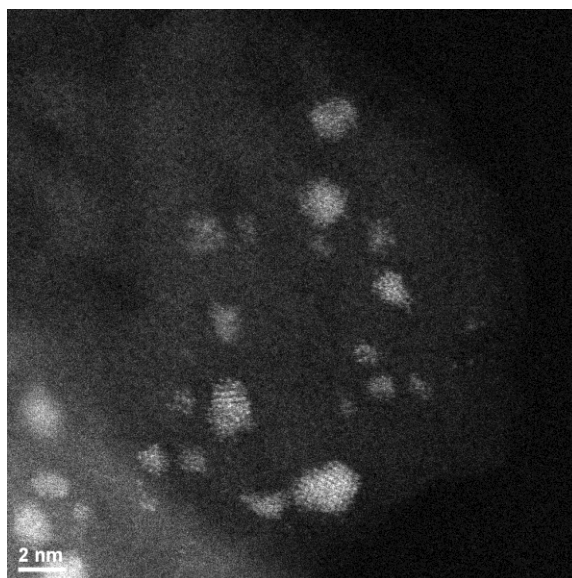


Figure S2. An HAADF - HRTEM image of Ir_5Bi_3 nanoparticles on MCM-41 after use in catalysis. The particles were formed from **2** on the support by thermal pretreatment at 300 °C for 2 h.

Table S3. Four EDS Composition Analyses of Ir_5Bi_3 catalyst after use on MCM-41 support.

Spectrum	Ir Atomic %	95% confidence	Bi Atomic %	95% confidence
1	62.46	±1.72	37.54	±1.58
2	64.93	±5.1	35.07	±4.68
3	64.38	±5.8	35.62	±5.32
4	75.92	±8.08	24.08	±7.44

Synthesis and analysis of APB oxidant:

APB served as a solid source of oxygen, liberating peroxyacetic acid (PAA) in situ when dissolved in water, it was synthesized by adding 4 mL (36-40% in acetic acid, Sigma) of peroxyacetic acid (23 mmol) to a glass reactor, preheated to 30 °C. 2.0 g of ground sodium tetraborate anhydrous (10 mmol, Sigma) was slowly added, yielding a white gel, which stirred for 16 hours. The white powder formed was dried at 50 °C for 16 hours.

The PAA concentration of APB was determined through an iodometric titration. In a standard procedure 0.1 g of APB was dissolved in 10 ml solution of 0.6 M KI. This was then titrated against a 0.1 M solution of Na₂S₂O₃. The PAA content was then determined through the following equation:

$$\%PAA = \frac{\text{Final titre/ml} \times 0.38}{\text{Mass of APB/g}}$$

Catalyst Evaluations:

The catalysts were activated through calcination by using a mixture of 5% H₂/N₂ for two hours at the stated temperature, prior to the catalytic tests. The liquid-phase oxidations were performed in a glass reactor at 66 °C by using 15 mmol of 3-picoline, 3.5 mmol of monoglyme internal standard, the appropriate quantity of acetylperoxyborate (APB) to yield 5 mmol of PAA (3:1 substrate:oxidant ratio), 25 mL of water and 150 mg of catalyst. The reaction mixtures were analyzed by using a Clarus 400 gas chromatogram, employed with a FID detector, using an Elite 5 column; the peak areas were calibrated using authenticated standards to evaluate respective response factors. Mass-balances were determined using the internal standard calibration method and individual response factors (RF) were calculated to establish a material balance and account

for handling losses. A typical example ($\text{Ir}_5\text{Bi}_3/\text{MCM-41}$, calcined at 300°C , 15 minute data point) is shown below.

Mass balance

RF for 3-Picoline (relative to Monoglyme)	2.0165
RF for Niacin (relative to Monoglyme)	1.17
Initial Monoglyme area	114612.2
Initial 3-Picoline area	1161982
Initial Niacin area	0
Initial moles of Monoglyme (added)	0.003329
Initial moles of 3-Picoline (detected)	0.016737
Initial moles of Niacin (detected)	0
Total initial reaction mix moles (detected)	0.016737
15 minutes Monoglyme area	69917.31
15 minutes 3-Picoline area	666737.9
15 minutes Niacin area	25325.5
15 mins moles of Monoglyme (added)	0.003329
15 mins moles of 3-Picoline (detected)	0.015742
15 mins moles of Niacin (detected)	0.001031
Total 15 mins reaction mix moles (detected)	0.016773
Mass balance	100.22
Conversion accounting for mole ratio	18.4
Niacin selectivity	99.9

The conversions were calculated as the percentage moles of picoline consumed, and these values were normalized relative to the oxidant ratio employed. Selectivity values were calculated from the moles of niacin produced, as a function of the total moles of product formed in mole percent. Turnover numbers (TON) were evaluated from the moles of picoline reacted per mole of the bimetallic catalyst Ir_3Bi or Ir_5Bi_3 .⁴

The effect of mesoporous support was investigated (Figure S3) by comparing a range of ordered and disordered mesoporous architectures. It was found that the choice of support has very little effect on the overall activity of the catalyst, though it plays a significant role in the observed niacin selectivity. Given that an analogous synthetic strategy was adopted using the (same) Ir₃Bi cluster and the fact that the pore dimensions of the mesopore are large enough to influence any diffusion restrictions, we can attribute the differences in catalytic selectivity to the surface-specific interactions between the cluster and support. The increased selectivity of the MCM-41 matrix makes it the preferred candidate for further optimizing the catalytic potential, due to the favorable catalyst-surface interactions. It is well known⁴ that the abundance of pendant silanol groups on the MCM-41 facilitate robust covalent anchoring of the cluster precursor, that leads to the creation of well-isolated single-sites.

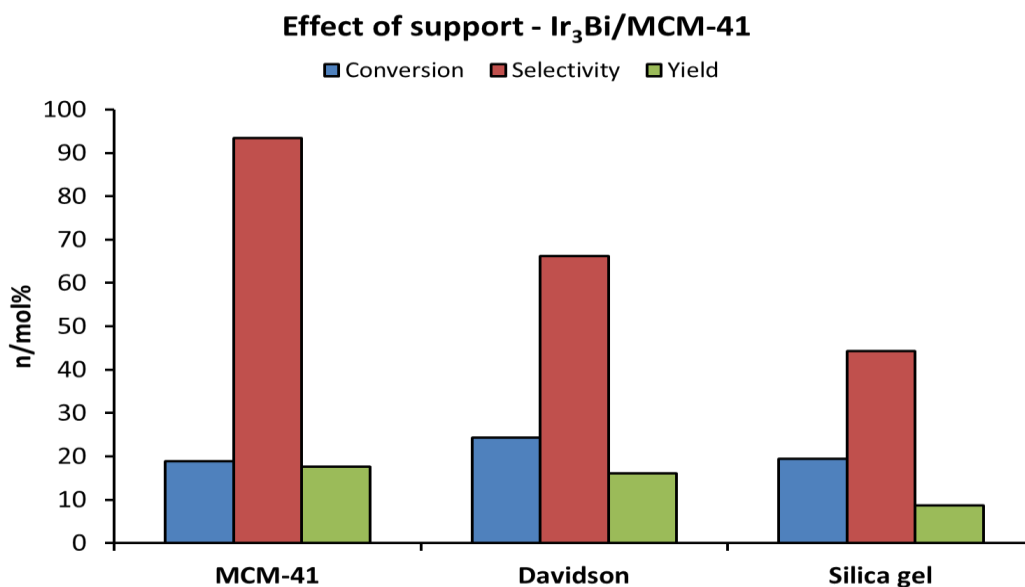


Fig S3: The effect of support in the oxidation of 3-picoline with Ir₃Bi. Reaction conditions: 15 mmol of 3-picoline, 3:1 molar ratio of picoline:peroxyacetic acid (derived from APB), 25 ml of H₂O, 150 mg of catalyst, 3.5 mmol of monoglyme internal standard, 65 °C, 45 minutes.

The complete removal of CO ligands is paramount to increasing the overall catalytic activity of these catalysts; as this facilitates a greater interaction of substrate and oxidant with the individual metal sites. A direct correlation can be observed between calcination temperature and degree of conversion of 3-picoline (Figure S4), which can be attributed to the removal of excess ligands and adsorbed molecules via calcination; making the catalytic active sites more readily accessible for oxidants and reactants. The selectivity is also greatly affected by the calcination temperature. Whilst there is very little change between 200-300 °C, on activation at 400 °C, the selectivity to niacin is significantly reduced, which strongly indicates that the catalytically active sites undergo sintering and subsequent aggregation at this temperature. It is highly likely that the structural integrity of the cluster is lost on sintering and thus the proximity of the metals is altered, thereby modifying the interaction of the different catalytic pathways.

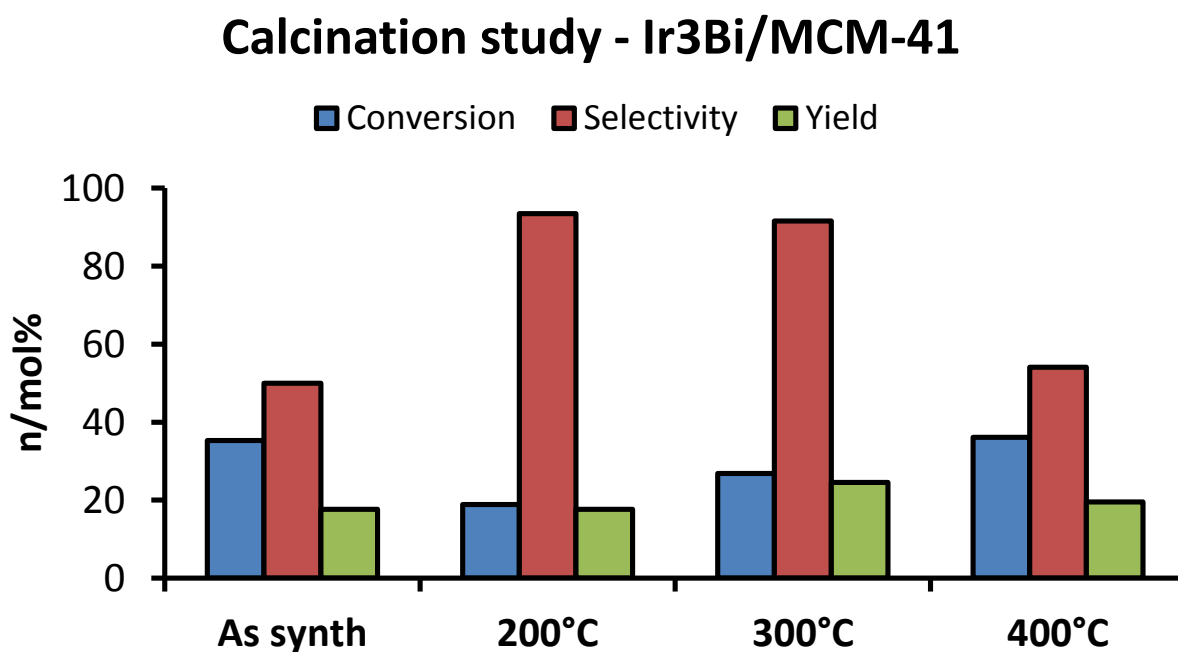


Figure S4: The effect of different calcination temperatures on the activity and selectivity of the Ir₃Bi/MCM-41 catalyst. Reaction conditions: 15 mmol of 3-picoline, 3:1 molar ratio of

picoline:peroxyacetic acid (derived from APB), 25 ml of H₂O, 150 mg of catalyst, 3.5 mmol of monoglyme internal standard, 65 °C, 45 minutes.

The structural and compositional integrity and heterogeneous nature of the Ir and Bi bimetallic clusters was confirmed by evaluating their recycle profile (Figure S5). Despite multiple reaction cycles, a constant catalytic profile was maintained, thereby confirming the resilience of the anchoring technique employed to anchor the catalysts to the inorganic support. While this confirms the heterogeneous nature of the materials, analysis of the reaction mixture, post catalysis, revealed < 3 ppb of any dissolved metal (Ir and Bi), which further emphasizes the synergistic importance of having isolated single-sites for enhancing the catalytic efficiency.

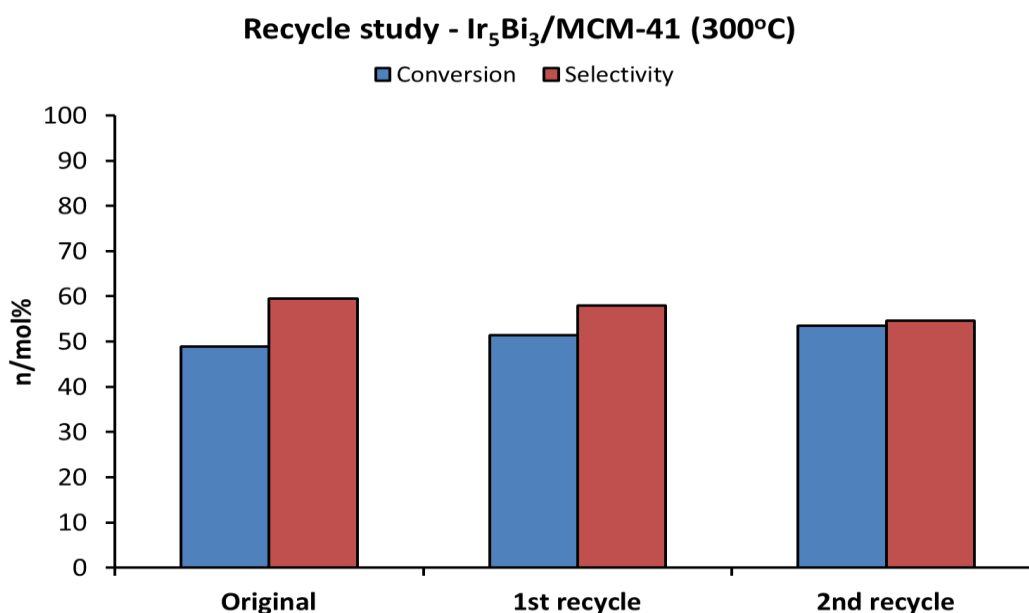


Figure S5: Catalyst recycle studies emphasizing the heterogeneous nature and recyclability of the anchored Ir₅Bi₃ catalyst. Reaction conditions: 15 mmol of 3-picoline, 3:1 molar ratio of picoline:peroxyacetic acid (derived from APB), 25 ml of H₂O, 150 mg of catalyst, 3.5 mmol of monoglyme internal standard, 65 °C, 45 minutes.

The effect of substrate:oxidant mole ratio was explored with a view to increasing the overall conversion of 3-picoline and corresponding yield of niacin, see Figure S6. It was observed that increasing the amount of oxidant saturates the individual metal sites, amplifying the available concentration and quantity of highly active oxidant intermediates with respect to the substrate, which subsequently blocks the 3-picoline molecules from accessing the active sites. This results in the wasteful decomposition of the oxidant that leads to the formation of the undesired N-oxides, while the pathway to niacin is greatly retarded. Due to the greater availability of the oxidant in the vicinity of the active site, the oxidant decomposition pathway predominates leading to a lower selectivity in the reaction. By limiting the oxidant ratio, the Ir sites are readily available for interaction with the 3-picoline, with the Bi sites preferentially activating and binding to the oxidant, that leads to a synergistic enhancement and concomitant increase in niacin selectivity.

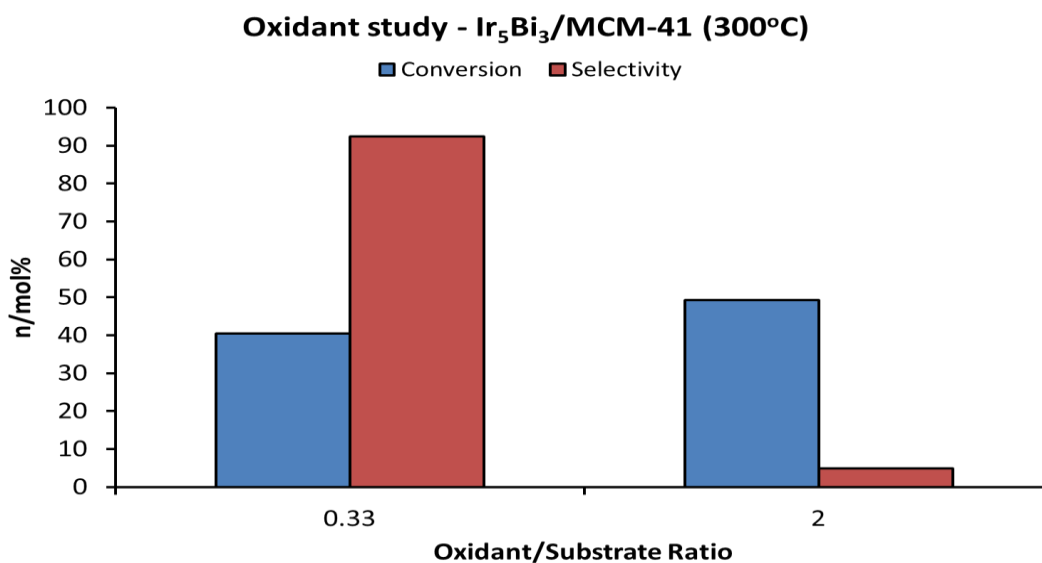


Figure S6: The effect of substrate:oxidant mole ratio on the activity and selectivity of the Ir₅Bi₃ catalyst for the oxidation of 3-picoline. Reaction conditions: 15 mmol of 3-picoline, 3:1 molar

ratio of picoline:peroxyacetic acid (derived from APB), 25 ml of H₂O, 150 mg of catalyst, 3.5 mmol of monoglyme internal standard, 65 °C, 45 minutes.

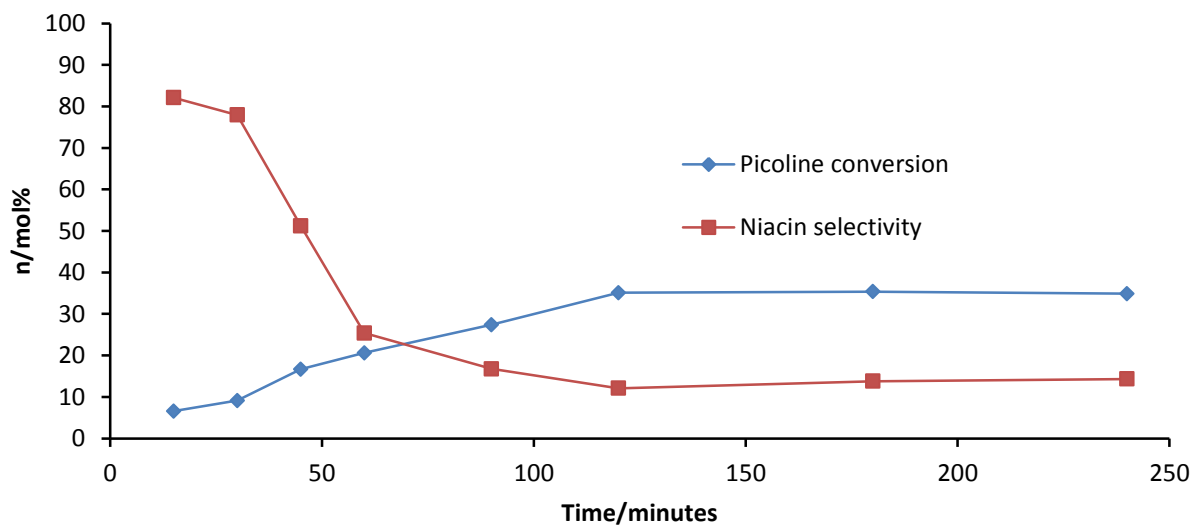


Figure S7: Kinetic plot for Ir/MCM-41, calcined at 300°C. Reaction conditions: 15 mmol of 3-picoline, 3:1 molar ratio of picoline:peroxyacetic acid (derived from APB), 25 ml of H₂O, 150 mg of catalyst, 3.5 mmol of monoglyme internal standard, 65 °C, 45 minutes.

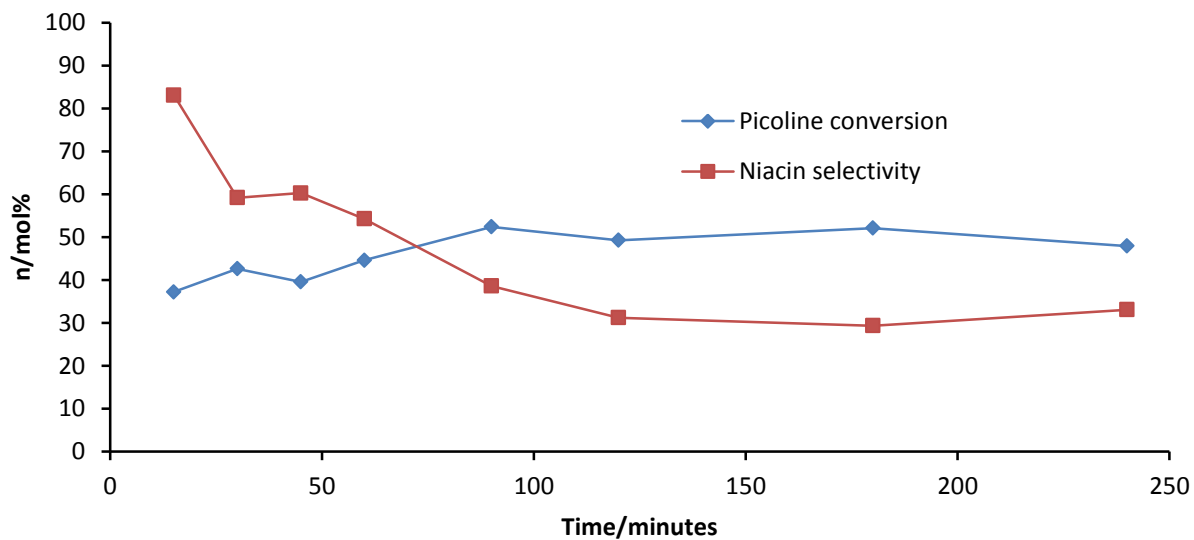


Figure S8: Kinetic plot for Bi/MCM-41, calcined at 300°C. Reaction conditions: 15 mmol of 3-picoline, 3:1 molar ratio of picoline:peroxyacetic acid (derived from APB), 25 ml of H₂O, 150 mg of catalyst, 3.5 mmol of monoglyme internal standard, 65 °C, 45 minutes.

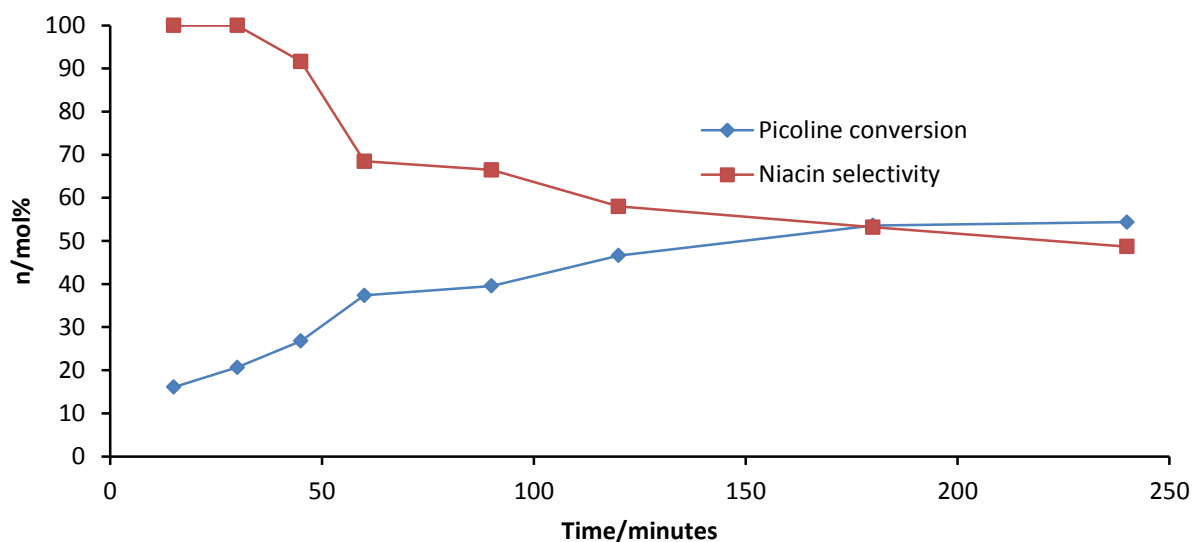


Figure S9: Kinetic plot for Ir₃Bi/MCM-41, calcined at 300°C. Reaction conditions: 15 mmol of 3-picoline, 3:1 molar ratio of picoline:peroxyacetic acid (derived from APB), 25 ml of H₂O, 150 mg of catalyst, 3.5 mmol of monoglyme internal standard, 65 °C, 45 minutes.

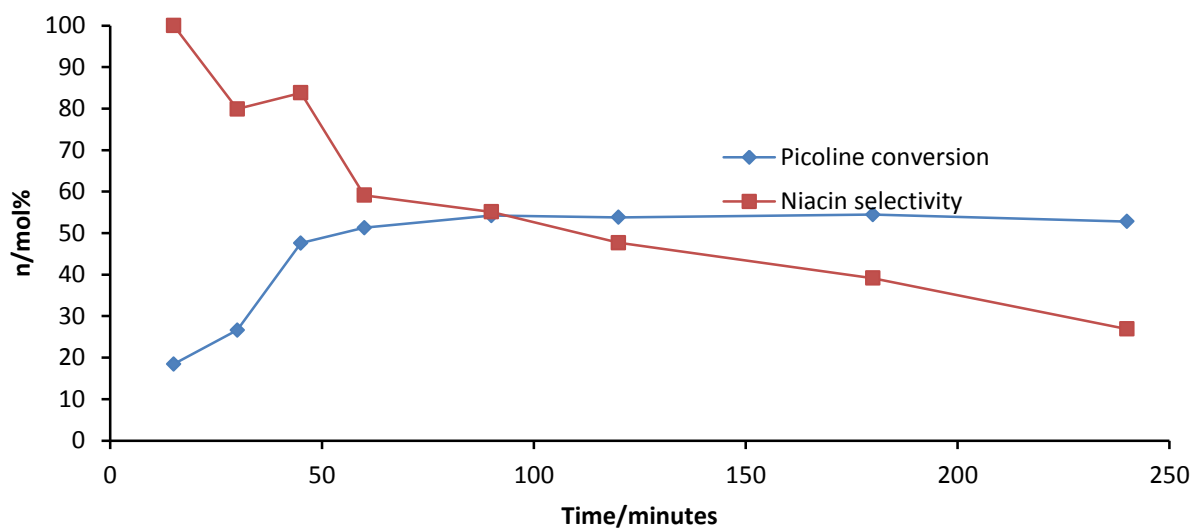


Figure S10: Kinetic plot for Ir₅Bi₃/MCM-41, calcined at 300°C. Reaction conditions: 15 mmol of 3-picoline, 3:1 molar ratio of picoline:peroxyacetic acid (derived from APB), 25 ml of H₂O, 150 mg of catalyst, 3.5 mmol of monoglyme internal standard, 65 °C, 45 minutes.

References

- 1) Adams, R. D.; Chen, M.; Elpitiya, G.; Zhang, Q. *Organometallics* **2012**, *31*, 7264-7271.
- 2) SAINT+, version 6.2a, Bruker Analytical X-ray Systems, Inc., Madison, WI, 2001.
- 3) G. M. Sheldrick, SHELXTL, version 6.1, Bruker Analytical X-ray Systems, Inc., Madison, WI, 1997.
- 4) Hungria, A. B.; Raja, R.; Adams, R.D.; Captain, B.; Thomas, J. M.; Midgley, P. A.; Golovko, V; Johnson, B. F. G.; *Angew. Chem. Int. Ed.*, **2006**, *45*, 4782-4785.